CPV Module to Rate Antireflective and Encapsulant Coating in Outdoor Conditions

A. Ritou, P. St Pierre, P.O. Provost, G. Forcade, C. Dubuc, O. Dellea, G. Hamon, M. Volatier, A. Jaouad, Christopher E. Valdivia, et al.

CPV Module to Rate Antireflective and Encapsulant Coating in Outdoor Conditions

Arnaud Ritou[1], Philippe St-Pierre[1], P.O. Provost[1], Gavin Forcade[2], Christian Dubuc[3], Olivier Dellea[4], Gwenaëlle Hamon[1], Maïté Volatier[1], Abdelatif Jaouad[1], Christopher E. Valdivia[2], Karin Hinzer[2], Vincent Aimez[1], Maxime Darnon[1,a)]

[1] Laboratoire Nanotechnologies Nanosystèmes (LN2) - CNRS IRL-3463 Institut Interdisciplinaire d'Innovation Technologique (3IT), Université de Sherbrooke, 3000 Boulevard Université, Sherbrooke, J1K 0A5 Québec, Canada
[2] SUNLAB, Centre for Research in Photonics, University of Ottawa, 25 Templeton St., Ottawa, Ontario, Canada, K1N 6N5
[3] Saint-Augustin Canada Electric Inc., Innovation and development of solar product, 75 rue d'Anvers, Saint-Augustin, Quebec Canada, G3A 1S5
[4] Grenoble Alpes Univ., CEA-Liten, 17 rue des Martyrs, 38054 Grenoble, France

[a)] Corresponding author: maxime.darnon@usherbrooke.ca

Abstract. Reflections are the most important channel losses in CPV modules. Since high efficiency solar cells need a protection against moisture and oxidation, we study an antireflective coating which also encapsulates the solar cells. It is based on a monolayer of microbeads partially submerged into PDMS. In this work, a CPV module is designed to compare the electrical performance of encapsulated and bare solar cells. A preliminary study demonstrates an increase in short-circuit current by 3.8% with EQE measurements and simulations. Outdoor measurements in Sherbrooke, Quebec, Canada gave a 6.4% increase in current for a 280X module on a clear cold day in September, after rejecting aberrant measurements, which confirms the interest of using microbeads as an antireflective coating for CPV applications.

INTRODUCTION

Concentrator photovoltaic (CPV) module are based on concentrating optics and multijunction solar cells. CPV module efficiency is almost twice the efficiency of the standard c-Si solar panels, but there is still an important gap between the solar cell efficiency and the final module efficiency. As an example, four-junction solar cells can reach 44% efficiency, but its highest module efficiency reached 38.9% efficiency [1]. To reduce this gap, we propose to enhance the optical efficiency by adding an antireflective coating to the encapsulant that protects the solar cell against humidity and oxidation. As Garcia-Linares *et al.* identified previously, a self-assembled layer of silica microbeads improves the light collection at the surface of the solar cell and is compatible with any type of surface covering the solar cell [2]. This microbead layer is similar to a moth-eye structure which acts as a antireflective coating (ARC) by smoothing the effective refractive index as represented in the FIGURE 1.b) [3]. In our case the microbeads are partially submerged into a PDMS layer which is the encapsulant of the solar cell. FIGURE 1.a) and b) represent a schematic view and SEM image, respectively, on which we define the submergence depth parameter. The enhancement of the light transmission thanks to the microbead ARC is demonstrated with a numerical model and validated by EQE measurements of triple junction solar cells (3JSC) with the structure described in FIGURE 2. Then we present a method to rate this ARC into a CPV module in outdoor conditions.

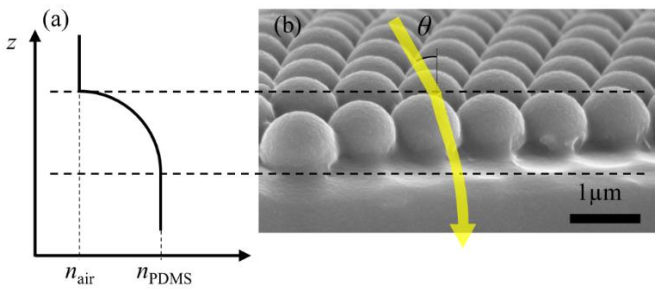

FIGURE 1. a) Empirical representation of the effective refractive index through the beads layer, b) SEM image of 1000 nm-diameter beads submerged by 25% of their diameter into PDMS with a representation of the optical path.

PRELIMINARY STUDY

Based on IQE and reflectivity measurements, we developed and validated the numerical model of our beads/PDMS/3JSC optical structure. In summary, this model calculates the J_{sc} as function of the bead diameter and submergence, defined as the percentage of bead diameter submerged into the PDMS. In the reference [4], we study the effect of the microbead pattern on the transmittance at the Air-Bead-PDMS interface at normal and inclined incidence. The theoretical maximum increase in J_{sc} is obtained for 760 nm bead diameter with 60% of submergence. In parallel, the beads/PDMS/3JSC real devices are also characterized by EQE measurements at 25°C and compared to the devices without beads and PDMS. Their J_{sc} are calculated by convolution of the EQE with the AM1.5D spectrum and the J_{sc} gain, noted ΔJ_{sc}, is calculated as follows:

$$\Delta J_{sc} = \frac{J_{sc}^{Beads} - J_{sc}^{Nobead}}{J_{sc}^{Nobead}} \quad (1)$$

For this study, the available bead diameter is 1000 nm and the achieved submergence is 25%. FIGURE 2 displays the EQE of the top and middle subcells of two representative devices in the eight considered in this study. The *"Beads" device* is the first device coated with PDMS and microbeads in the 280X sub-module (see below). It produces 13.4 mA/cm² with its top subcell and 13.2 mA/cm² with its middle subcell. The *"NoBead" device* is the first device uncoated in the 280X sub-module which produces 12.7 mA/cm² and 12.8 mA/cm² with its top and middle subcells, respectively. Comparing 280X-bead#1 to 280X-nobead#1 with Eq. (1), we calculate ΔJ_{sc} = +3.2% for the current limiting middle subcell and ΔJ_{sc} = +5.6% for the top subcell.

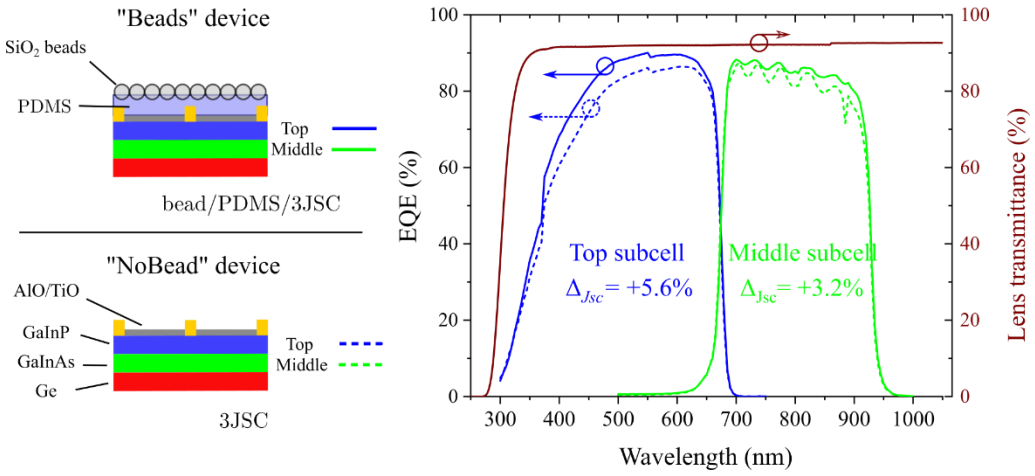

FIGURE 2. Description of the two different devices structures with their EQE measurement at 25°C and the n-BK7 lens material transmittance.

The numerical model gives ΔJ_{sc} = +3.7% for 1000 nm-diameter beads submerged 25% into the PDMS in comparison to the identical cell without beads nor PDMS. Comparing the EQE-derived J_{sc} averaged over four fabricated devices each, the bead/PDMS/3JSC devices give a ΔJ_{sc} = +3.9% in comparison to the bare 3JSC.

Finally, our EQE measurements are very close from the numerical model, for one sun concentration, AM1.5D spectrum and 25°C. Now we want to compare the performances of coated vs uncoated receivers in a CPV module in outdoor conditions with concentrating optics.

OUTDOOR EXPERIMENTAL STUDY

Experimental outdoor characterization method

To unify electrical connections and thermal behavior of the PV devices, all the 3JSC are packaged on an aluminum substrate. Half of them are coated by spinning a droplet of PDMS at 6,000 rpm for 120s to obtain a 6 µm-thick layer. Then the PDMS is cured at 125°C during a fraction of the total curing time of the PDMS. Thus, we control the partial submergence of the beads. The eight receivers manufactured are split into two different CPV-modules, 280X and 500X geometric concentrating ratios. The 280X uses Thorlabs glass aspheric lenses for which the n-BK7 material transmittance is plotted for a 10mm thick flat sample in the **FIGURE 2**. The 500X uses silicone-on-glass Fresnel lenses from STACE. As is represented in FIGURE 3, the focal length of both modules is fixed but the receivers can move in two directions in the focal plane of the lenses with a micrometric resolution. Each receiver has a thermocouple placed under one fixing screw to monitor its temperature. We also monitor the lens's temperature by gluing a thermocouple to the aluminum holding plate of each 4-element module. Finally, an alignment test pattern allows to visualize the tracking accuracy.

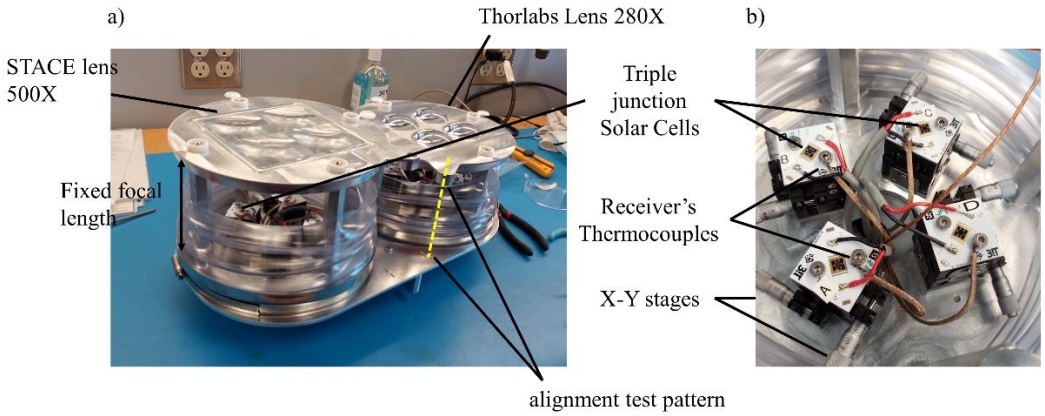

FIGURE 3. a) Photo of the CPV module with 500X and 280X sub-modules. b) Configuration of the four-receivers of one sub-module.

The CPV module is installed on a two-axis tracker with ±0.01° tracking accuracy. While the CPV modules are pointing at the sun, we manually adjusted the X-Y receiver position to have the light spot totally comprised onto the solar cell area, by visual inspection. To control the alignment of the receivers we run a test protocol with the tracker to determine the angular acceptance of every mono-module. While we voluntary add a random angular offset to the tracker, we monitor the maximum power (P_{mp}) of every receiver simultaneously with the direct normal irradiance (DNI) taken on another tracker situated in the solar park of the 3IT. By doing this every minute in a day without clouds, we can represent the angular acceptance map displayed in the FIGURE 4. In these maps, each colored hexagon represents the P_{mp} divided by the DNI for the corresponding azimuthal and elevation tracking offset angle. Because it is a random angular offset, the points measured several times are averaged and the empty points are left blank. The grey crosses represent the centroid of the angular map. If the centroid is contained in the black circle which represent the arbitrary offset angle target of the monomodules, we considered the X-Y alignment of the receivers acceptable for inter-comparison. For example, the *500X-beads#2* and *280X-nobeads#2* receivers are not properly aligned and will be excluded from the comparison study. In the 500X module, we see a variation of P_{mp}/DNI ratio that we assume to come

from the variation of optical efficiency from lens to lens. Finally, the influence of the beads/PDMS encapsulant and ARC is studied just for the 280X sub-module in the upcoming paragraph.

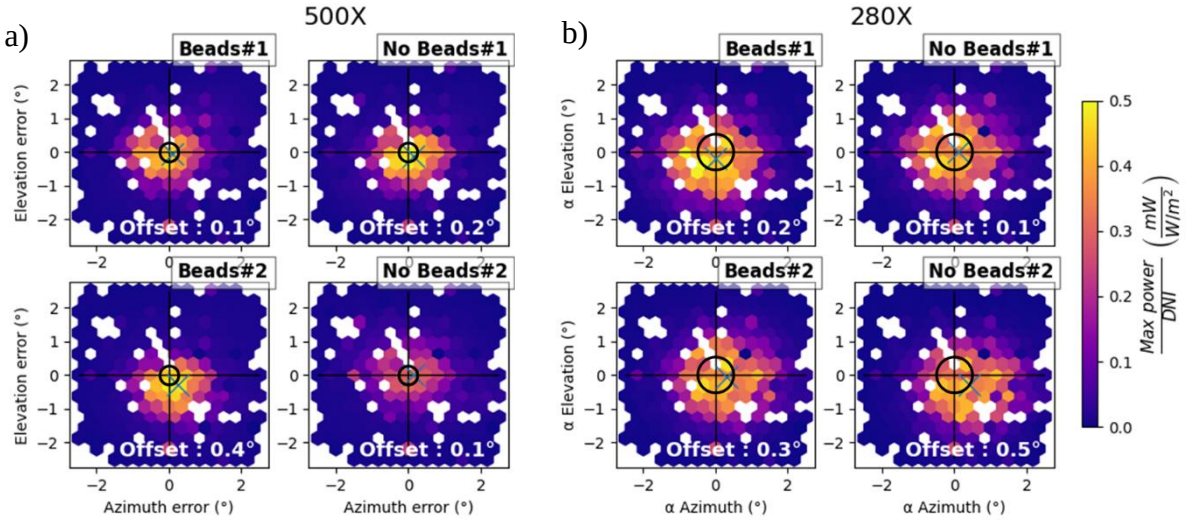

FIGURE 4. Angular acceptance map of : a) the four 500X monomodules with silicone-on-glass Fresnel lenses, b) the four monomodules with 280X aspheric glass lenses. Black circles represent the acceptance angles, grey crosses the centroid of each map.

280X module outdoor performances

The outdoor measurement period was in September 2020, which was a particularly cloudy month at Sherbrooke, Canada. Between the 3rd to the 20th we chose the clearest day to analyze the performances of the four monomodules with 280X concentrating ratio, which was the 18th. FIGURE 5 represents the I_{sc} as function of the DNI for the two receivers with microbeads and PDMS ARC and the two receivers without. We see that the highest currents correspond to the coated receiver, in accordance with the preliminary study. The misaligned receiver, the *280X-Beads#2* has lower current, in accordance with the acceptance maps of FIGURE 4. For a DNI equal to $900^{\pm 10}$ W/m², the averaged J_{sc} is 202 mA for the *280X-beads#1* monomodule and 190 mA for the *280X-nobead#1* monomodule. This induces a ΔJ_{sc} = +6.4%, which is almost twice the measured ΔJ_{sc} with EQE at 25°C with AM1.5D spectrum and 1X concentration. The outdoor measurements are done with an average ambient temperature of 12°C, lens temperature of 19°C, and receiver temperature of 32°C. However, we did not monitor the solar spectrum we did not monitor the solar spectrum received by the solar cell, which will differ from the standard AM1.5D spectrum used to calculate the J_{sc} from the EQE measurements. The lenses will introduce both absorption and chromatic aberration into the system, although this is highly dependent upon the specific design of the optical train and materials employed, and therefore, was not included here for generality. Regarding the difference of ΔJ_{sc} from a subcell to another in FIGURE 2, the limiting subcell of the CPV module can become the top subcell if the solar spectrum becomes red-rich. In such a spectral condition, our indoor measurement showed a 5.6% intensity improvement with microbeads. Moreover, the indoor measurements are realized under normal incidence but the microbeads pattern also decreases the reflections when the light incident angle increases [4]. The larger J_{sc} improvement in outdoor measurement compared to indoor measurements can therefore be attributed to (1) difference in solar spectrum that make the top cell limiting the short circuit current ; (2) the angular distribution of light incidence on the solar cell ; (3) difference in measurement temperature.

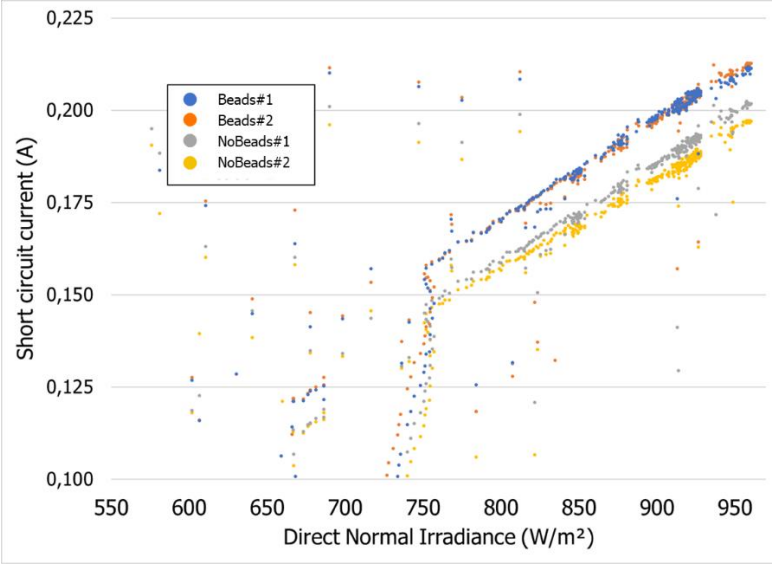

FIGURE 5. Short-circuit current of the four 280X monomodules as function of the direct irradiance.

CONCLUSION

We developed an encapsulant and ARC coating based on a patterned microbead layer. A validated numerical model of the optical structure shows an increase in short circuit current by 3.7%, compared to a bare triple junction solar cell. In addition, J_{sc} were calculated from AM1.5D spectrum and EQE measurement for the 8 devices used in a CPV module. Comparing the average current of the four encapsulated 3JSC to the four non-encapsulated cells, the ΔJ_{sc} is 3.9%, for 1X concentration, at 25°C. To confirm the increase in J_{sc} thanks to the microbead ARC, we designed and manufactured a CPV module with 500X and 280X sub-modules. After rejecting the aberrant results, the increase in J_{sc} is still positive with almost twice the ΔJ_{sc} at 6.4%. TABLE 1 below summarizes the ΔJ_{sc} obtained with the three methods to rate the optical efficiency of the microbead and PDMS ARC and encapsulant. The large increase in J_{sc} observed in the 280X CPV module could be enhanced by the spectral variations. If the spectrum is red-rich, the top subcell should become current limiting, for which we measured an increase in J_{sc} by +5.6% from EQE measurements in standard conditions.

TABLE 1. ΔJ_{sc} calculated with numerical model, EQE measurement and Outdoor characterization in the 280X CPV module.

	Numerical model	**EQE**	**CPV Module**
ΔJ_{sc}	+3,7%	+3,9%	+6,4%
Conditions	1X, 900W/m², 25°C, AM1.5D	1X, 900W/m², 25°C, AM1,5D	280X, $900^{\pm 10}$ W/cm², 12 - 32°C unknown spectrum

ACKNOWLEDGMENTS

We acknowledge the support from STACE, MITACS and Quebec Ministère de l'Économie et de l'Innovation. LN2 is a joint International Research Laboratory (IRL 3463) funded and co-operated in Canada by Université de Sherbrooke (UdeS) and in France by CNRS as well as Ecole Centrale Lyon (ECL), Institut National des Sciences Appliques (INSA Lyon) and Université Grenoble Alpes (UGA). It is also supported by the Fonds de Recherche du Québec Nature et Technologie (FRQNT).

REFERENCES

[1] S. van Riesen *et al.*, « New module design with 4-junction solar cells for high efficiencies », *AIP Conf. Proc.*, vol. 1679, nº 1, p. 100006, sept. 2015, doi: 10.1063/1.4931553.

[2] P. García-Linares *et al.*, « Improving optical performance of concentrator cells by means of a deposited nanopattern layer », *AIP Conf. Proc.*, vol. 1679, nº 1, p. 040004, sept. 2015, doi: 10.1063/1.4931515.

[3] H. K. Raut, V. A. Ganesh, A. S. Nair, et S. Ramakrishna, « Anti-reflective coatings: A critical, in-depth review », *Energy Environ. Sci.*, vol. 4, nº 10, p. 3779-3804, sept. 2011, doi: 10.1039/C1EE01297E.

[4] G. Forcade *et al.*, « Nanostructured surface for extended temperature operating range in concentrator photovoltaic modules », *AIP Conf. Proc.*, vol. 2298, nº 1, p. 050002, nov. 2020, doi: 10.1063/5.0032134.